NUREG/CR-0169
VOL. V
TREE-1089
for U.S. Nuclear Regulatory Commission

# LOFT EXPERIMENTAL MEASUREMENTS UNCERTAINTY ANALYSES

## VOLUME V

## LOFT EXTERNAL ACCELEROMETER UNCERTAINTY ANALYSIS

PATRICK A. QUINN GARRE L. BILADEAU
ROBERT Y. MAUGHAN

October 1978

EG&G Idaho, Inc.

IDAHO NATIONAL ENGINEERING LABORATORY

DEPARTMENT OF ENERGY

IDAHO OPERATIONS OFFICE UNDER CONTRACT EY-76-C-07-1570

7812220 0343

NOTICE

This report was prepared as an account of work sponsored by an agency of the United States Government. Neither the United States Government nor any agency thereof, or any of their employees, makes any warranty, expressed or implied, or assumes any legal liability or responsibility for any third party's use, or the results of such use, of any information, apparatus, product or process disclosed in this report, or represents that its use by such third party would not infringe privately owned rights.

The views expressed in this report are not necessarily those of the U.S. Nuclear Regulatory Commission.

Available from
National Technical Information Service
Springfield, Virginia 22161
Price: Printed Copy A03; Microfiche $3.00

The price of this document for requesters outside the North American continent can be obtained from the National Technical Information Service.

NUREG/CR-0169
TREE-1089
Vol. V
R2

# LOFT MEASUREMENTS UNCERTAINTY ANALYSES
## VOLUME V
## LOFT EXTERNAL ACCELEROMETER UNCERTAINTY ANALYSIS

Patrick A. Quinn
Garre L. Biladeau
Robert Y. Maughan

EG&G Idaho, Inc.
Idaho Falls, Idaho 83401

Date published: October 1978

PREPARED FOR THE
U.S. NUCLEAR REGULATORY COMMISSION
AND THE U.S. DEPARTMENT OF ENERGY
IDAHO OPERATIONS OFFICE
UNDER CONTRACT NO. EY-76-C-07-1570
NRC FIN No. A6043

# ABSTRACT

A performance analysis of the loss-of-fluid test (LOFT) external accelerometer measurements is presented. Along with complete descriptions of test programs that have been conducted, specific sources of measurement uncertainty are identified, quantified, and combined to provide an assessment of the ability of this measurement to satisfy the requirement for measurement of structural acceleration.

The theoretical framework and general methods employed in this volume are discussed in NUREG/CR-0169, TREE-1089, Volume I, "Summary of LOFT Experimental Measurements Uncertainty Analyses".

This document supersedes LTR 141-39, Supplement Number 4. Four volumes of the TREE-1089 series were published prior to implementation of NUREG/CR numbering system. Volumes VI, IX, XV and XVI were published as TREE-NUREG-1089; the remaining volumes are published as NUREG/CR-0169, TREE-1089.

## SUMMARY

The evaluation of analytical techniques for predicting the response of reactor structures is essential for design and analysis of reactors and reactor safety systems. Accelerometers are one type of transducer used to obtain data for this evaluation.

Accelerometers used in the Loss-Of-Fluid Test (LOFT) Facility are the piezoelectric type manufactured by Gulton/Servonic. The output of the accelerometer goes to a charge amplifier whose output is recorded on the Data Acquisiton and Visual Display System wide-band frequency modulated channels.

The measurement uncertainty analysis showed the major sources of uncertainty in the accelerometer were the transverse sensitivity and calibration of the transducers. Anticipated dynamic base strains at two installations (AE-BL4-1 and AE-BL5-1) will cause a slight increase in the uncertainty of these two measurements. The balance of the accelerometers were isolated from change in base strain. The accuracy requirement as specified in the LOFT Measurement Requirements Document (MRD), is ±10% ot reading (RD) for accelerometers. Table IV shows that LOFT experimental accelerometer accuracies are ±4.6% RD plus (RSS) ±0.95 $m/s^2$ (95% confidence level) for the vessel bottom and LOFT test assembly (LTA). The accuracies are ±8.1% RD plus (RSS) ±0.95 $m/s^2$ for AE-BL-3-1, which is well within the requirement. The uncertainty of AE-BL4-1 and AE-BL5-1 is ±8.1% RD plus ±0.97 $m/s^2$ each. The expected rise time (0.35 ms) is within the MRD requirement (1.0 ms). The rise time of the accelerometer itself is 23 μs (15.2 kHz).

CONTENTS



FIGURES

TABLES

# LOFT EXTERNAL ACCELEROMETER UNCERTAINTY ANALYSIS

## I. INTRODUCTION

Measurement uncertainty analyses were performed to evaluate the anticipated performance uncertainty for each experimental measurement made in the Loss-of-Fluid Test (LOFT) facility[1]. Results of these analyses are reported in a series of volumes to NUREG/CR-0169, TREE-1089[a]. Volume I[2] of this series describes the LOFT experimental measurement system and the technique used for calculating the uncertainties and includes a summary of each uncertainty analysis. The remaining volumes in the series present detailed results from the uncertainty analysis performed for each experimental measurement.

The evaluation of analytical techniques for predicting the response of reactor structures is essential to (a) the design and analysis of reactor safety systems, (b) the analysis of reactor structural response to accidental loadings, such as earthquakes and subcooled decompression; and (c) the analysis or design specification of components within a reactor system. The theoretical basis for the computer programs employed to predict the response of reactor structures is well established. Hence, the emphasis for reactor structural analyses is on evaluation of modeling techniques, on determination of the number of modes of vibration which must be represented to adequately define the response of a system, and on the technique for applying the forcing function to the analytical model evaluated[1].

---

[a] Volumes VI, IX, XV, and XVI were published prior to implementation of the NUREG/CR numbering system as TREE-NUREG-1089; all remaining volumes will be published as NUREG/CR-0169, TREE-1089.

## II. DESCRIPTION

There are a total of 39 external accelerometer measurements (see Table I), divided into two categories:

(1) Thirty-three on the LOFT test assembly (LTA), located on the primary coolant, blowdown, and reactor vessel systems (see Figure 1).

(2) Six on the reactor vessel bottom (AC-RV1-1 through AC-RV1-6) (see Figure 2).

The accelerometers are piezoelectric from Gulton/Servonic: six AQB-10180088 ultra-high-temperature accelerometers installed on the reactor vessel bottom and 33 ATP-10180134 accelerometers installed at various places on the LTA. Specifications are given in Appendix A.

The sensing element common to all acceleration transducers is the seismic mass (proof mass) contained in a damped spring-mass system. When acceleration is applied to the transducer case, the mass moves relative to the case. When the acceleration stops, the spring returns the mass to its original position.

Designs are typified as shown schematically in Figure 3. The acceleration sensing axis is perpendicular to the base. Crystals are polarized to minimize any output due to acceleration along any other axes. In all design versions, at least a portion of the spring action of the spring-mass system is provided by the crystal (C) itself.

TABLE I

ACCELEROMETER LISTINGS

| Number | Total | Location | Model Number |
|---|---|---|---|
| AE-RV2-1 | 1 | Reactor vessel (west side) | ATP-10180134 |
| AE-RV3-1 | 1 | Reactor vessel (south side) | ATP-10180134 |
| AE-RV4-1,-2, -3,-4 | 4 | Reactor vessel (north, east, south, and west side) | ATP-10180134 |
| AE-PC3-1, -2,-3 | 3 | 90° elbow, just downstream of pumps | ATP-10180134 |
| AE-PC6-1, -2,-3 | 3 | 135° elbow in operating loop between RV outlet nozzle and SG inlet nozzle | ATP-10180134 |
| AE-PC7-1, -2,-3 | 3 | 90° elbow in operating loop between RV outlet nozzle and SG inlet nozzle | ATP-10180134 |
| AE-PC10-1,-2 | 2 | Blowdown suppression tank | ATP-10180134 |
| AE-PC16-1, -2,-3 | 3 | Pump inlet nozzles | ATP-10180134 |
| AE-PC17-1,-2 | 2 | Steam generator (north side) | ATP-10180134 |
| AE-PC18-1, -2,-3 | 3 | Pump #1 (north side) | ATP-10180134 |
| AE-PC19-1, -2,-3 | 3 | Pump #2 (north side) | ATP-10180134 |
| AE-BL2-1,-2 | 2 | Steam generator simulator | ATP-10180134 |
| AE-BL3-1 | 1 | Steam generator simulator | ATP-10180134 |
| AE-BL4-1 | 1 | Quick-opening valve (east) | ATP-10180134 |
| AE-BL5-1 | 1 | Quick-opening valve (west) | ATP-10180134 |
| AE-RV1-1, -2,-3 | 3 | Reactor vessel bottom (0°) | AQB-10180088 |
| AE-RV1-4, -5,-6 | 3 | Reactor vessel bottom (90°) | AQB-10180088 |

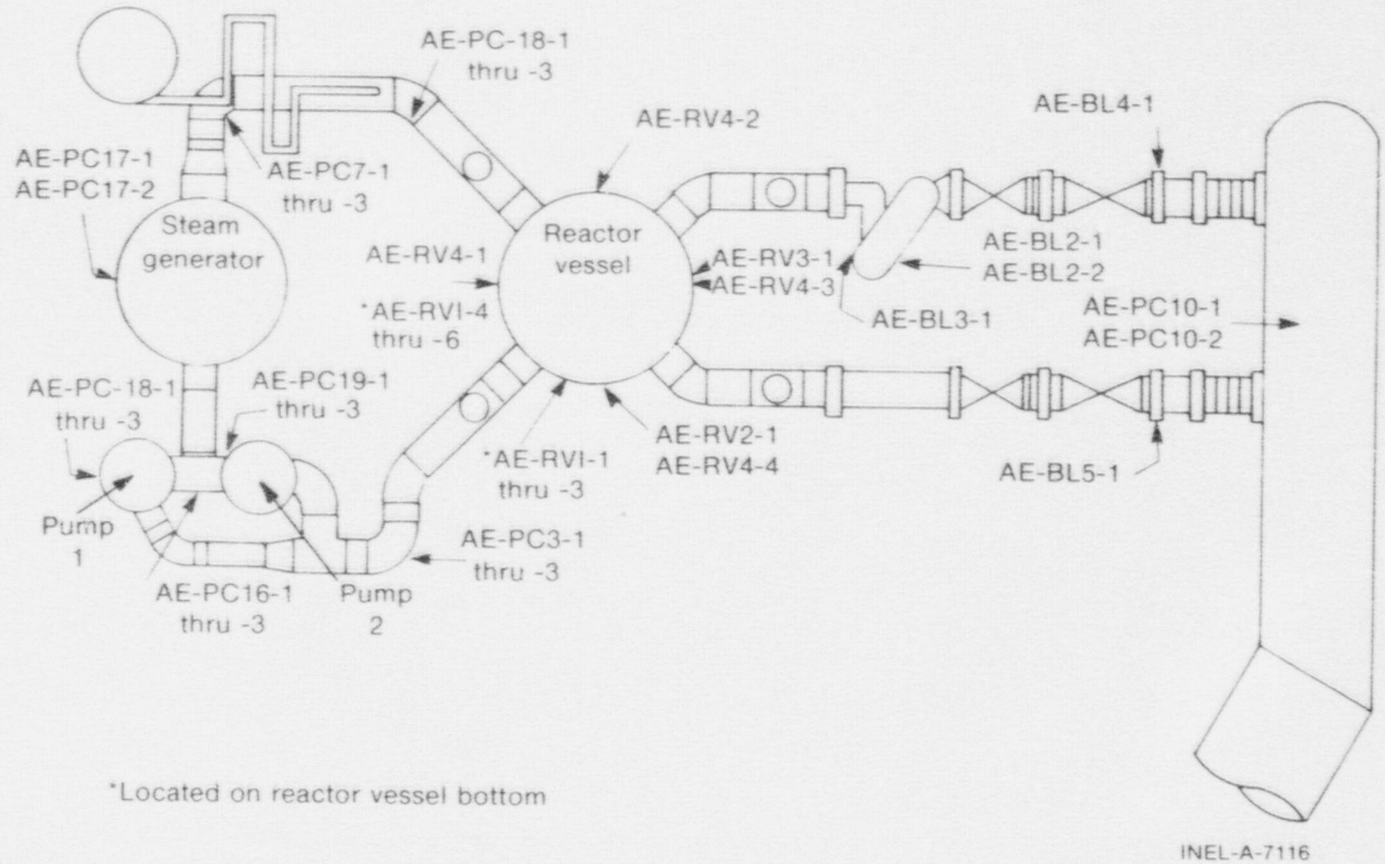


Fig. 1 External accelerometer locations.

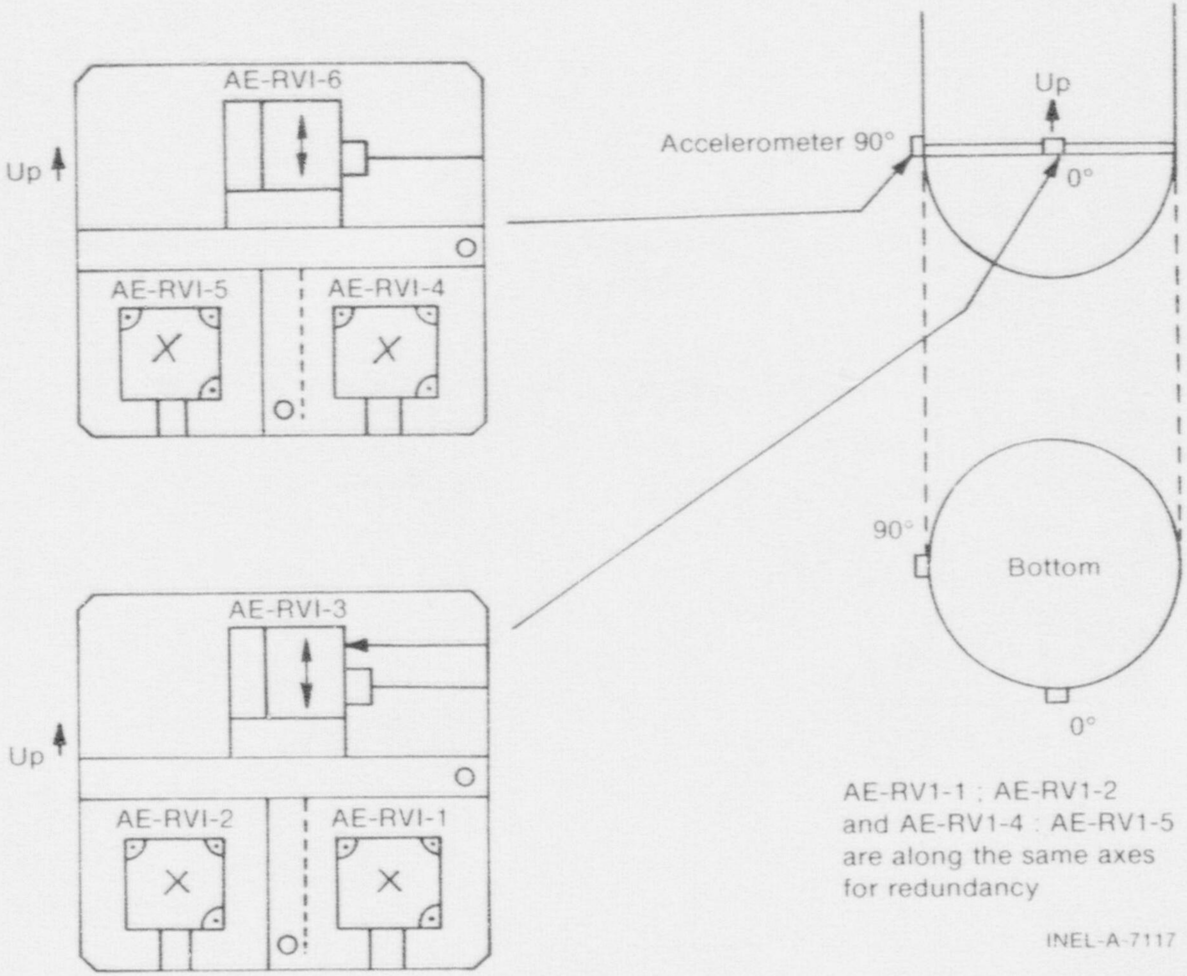


Fig. 2 External accelerometer - reactor vessel bottom placement.

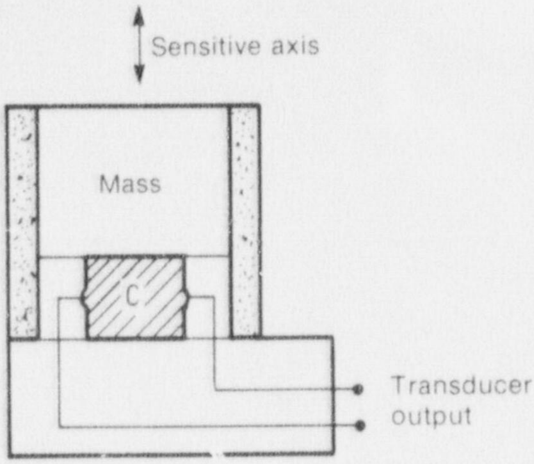


Fig. 3 Piezoelectric accelerometer.

The entire accelerometer measurement system as used in loss-of-fluid test (LOFT) is shown schematically in Figure 4. The data acquisiton and visual display system (DAVDS) portion of its measurement is evaluated in NUREG/CR-0169, TREE-1089, Volume II.

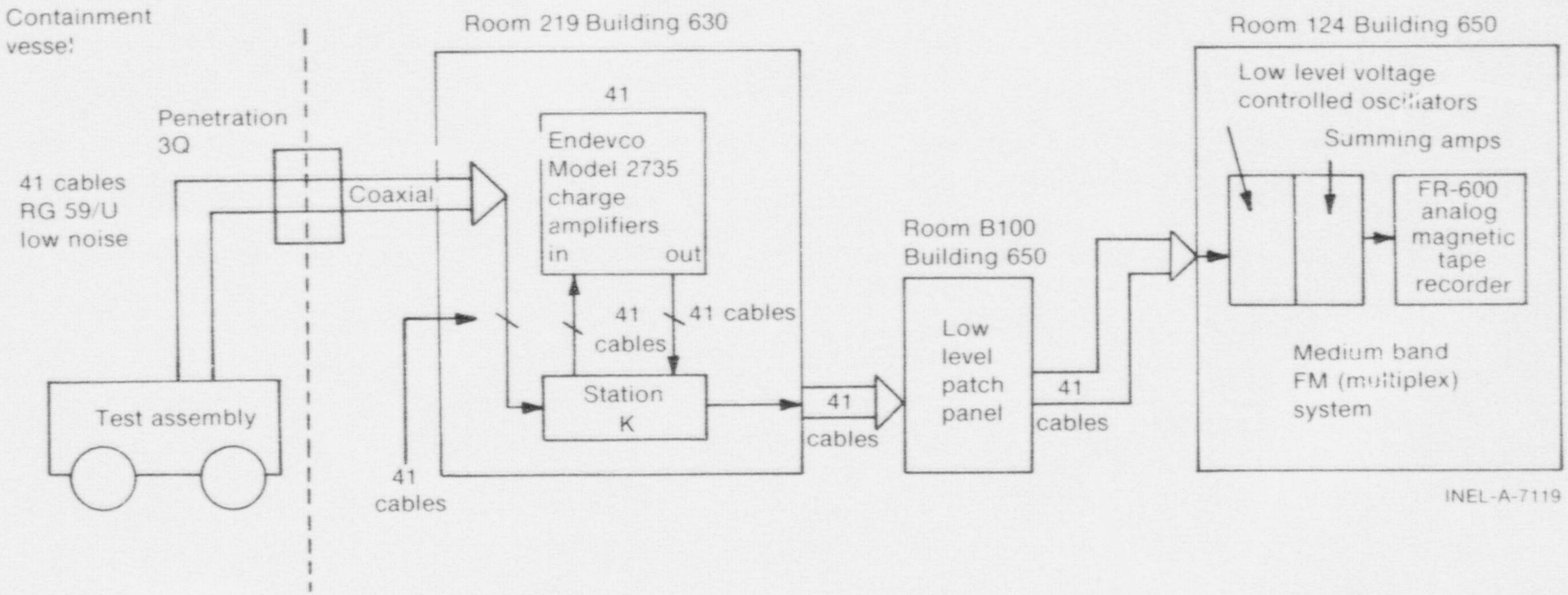


Fig. 4 LOFT external accelerometer measurement system.

## III. DISCUSSION OF SPECIFIC UNCERTAINTIES

### 1. SENSITIVITY TO EXTRANEOUS STIMULATION

#### 1.1 Transverse Axis Sensitivity

Accelerometers are designed to maximize transducer output along a specific axis while minimizing the output arising from acceleration along other (transverse) axes. Based on four measurements, (from vendor acceptance tests) the sensitivity o. either transverse axis is 2.6% of reading (RD) within an uncertainty limit of $\pm 0.56\%$ RD.

The output that the accelerometer will register is the magnitude of the acceleration vector sum reflected through the axis sensitivities. Equations of special interest are numbered.

For example, an accelcrometer with primary sensitivity in the x direction then,

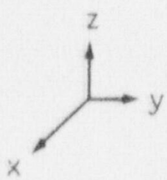


$$C_o = \left| \Sigma_{ox} a_x \hat{i} + \Sigma_{oy} a_y \hat{j} + \Sigma_{oz} a_z \hat{k} \right|$$

$\hat{i}$, $\hat{j}$, $\hat{k}$ are unit vectors in the i, j, and k directions, respectively.

$$C_o = \sqrt{(\Sigma_{ox} a_x)^2 + (\Sigma_{oy} a_y)^2 + (\Sigma_{oz} a_z)^2}$$

where,

$a_i$ = the acceleration in the i direction ($m/s^2$)

$\Sigma_{ik}$ = the acceleration sensitivity in the k direction ($pC \cdot s^2/m$) of the $i^{th}$ accelerometer

$C_i$ = the $i^{th}$ accelerometer output in picocoulombs (pC)

$S_k$ = the standard deviation of uncertainty for factor k.

Given three accelerometers with their sensitive axes in the x, y, and z directions (devices numbered 1, 2, and 3, respectively), then

$$C_1^2 = (\Sigma_{1x} a_x)^2 + (\Sigma_{1y} a_y)^2 + (\Sigma_{1z} a_z)^2$$

$$C_2^2 = (\Sigma_{2x} a_x)^2 + (\Sigma_{2y} a_y)^2 + (\Sigma_{2z} a_z)^2$$

$$C_3^2 = (\Sigma_{3x} a_x)^2 + (\Sigma_{3y} a_y)^2 + (\Sigma_{3z} a_z)^2.$$

$$\Sigma_{1x} \cong \Sigma_{2y} \cong \Sigma_{3z}$$

Others are about 2.6% of this (i.e., $\Sigma_{1y} \cong 0.026\Sigma_{1x}$).

$$\frac{C_1}{\Sigma_{1x}}, \ \frac{C_2}{\Sigma_{2y}} \text{ and } \frac{C_3}{\Sigma_{3z}}$$

are first order approximations to $a_x$, $a_y$ and $a_z$ respectively.

A better correction is

$$^*a_x = \frac{1}{\Sigma_{1x}} \sqrt{C_1^2 - \left(\frac{\Sigma_{1y} C_2}{\Sigma_{2y}}\right)^2 - \left(\frac{\Sigma_{1z} C_3}{\Sigma_{3z}}\right)^2}$$

$$^*a_y = \frac{1}{\Sigma_{2y}} \sqrt{C_2^2 - \left(\frac{\Sigma_{2x} C_1}{\Sigma_{1x}}\right)^2 - \left(\frac{\Sigma_{2z} C_3}{\Sigma_{3z}}\right)^2}$$

$$^*a_z = \frac{1}{\Sigma_{3z}} \sqrt{C_3^2 \left(\frac{\Sigma_{3x} C_1}{\Sigma_{1x}}\right)^2 - \left(\frac{\Sigma_{3y} C_3}{\Sigma_{2y}}\right)^2}$$

or

$$^*a_x = \frac{1}{\Sigma_{1x}} \sqrt{C_1^2 - (0.026\ C_2)^2 - (0.026\ C_3)^2} \qquad (1)$$

$$^*a_y = \frac{1}{\Sigma_{2y}} \sqrt{C_2^2 - (0.026\ C_1)^2 - (0.026\ C_3)^2} \qquad (2)$$

$$^*a_z = \frac{1}{\Sigma_{3z}} \sqrt{C_3^2 - (0.026\ C_1)^2 - (0.026\ C_2)^2} \qquad (3)$$

Since the transverse axis sensitivities are known to be 2.6% RD to within ±0.56% RD.

The uncertainty in $*a_x$, for example, as a result of the uncertainties in the values of the various transverse sensitivities can be expressed as follows:

$$\left(*a_x\right)^2 = \frac{1}{\left(\Sigma_{1x}\right)^2}\left|C_1{}^2 - (p_2C_2)^2 - (p_3C_3)^2\right|$$

where

$$p_2 = \Sigma_{1y}/\Sigma_{2y} \quad p_3 = \Sigma_{1z}/\Sigma_{3z}$$

$$2\left(*a_x\right)\frac{\partial\left(*a_x\right)}{\partial p_2} = \frac{-2C_2{}^2}{\left(\Sigma_{1x}\right)^2}\,p_2$$

$$2\left(*a_x\right)\frac{\partial\left(*a_x\right)}{\partial p_3} = \frac{-2C_3{}^2}{\left(\Sigma_{1x}\right)^2}\,p_3$$

since

$$\left|S\left(*a_x\right)\right|^2 = \left[\frac{\partial\left(*a_x\right)}{\partial p_2}\right]^2\left(S_{p_2}\right)^2 + \left[\frac{\partial\left(*a_x\right)}{\partial p_3}\right]^2\left(S_{p_3}\right)^2$$

then

$$= \left[\frac{C_2{}^2\ p_2}{*a_x\ \left(\Sigma_{1x}\right)^2}\right]^2\left(S_{p_2}\right)^2 + \left[\frac{C_3{}^2\ p_3}{*a_x\ \left(\Sigma_{1x}\right)^2}\right]^2\left(S_{p_3}\right)^2$$

but

$$\left(S_{p_2}\right)^2 \cong \left(S_{p_3}\right)^2 = S_p{}^2 = (0.0056)^2$$

and

$$p_2 \cong p_3 = p = (0.026)$$

so,

$$\left[S\left({}^{*}a_x\right)\right]^2 = \left[\frac{C_2^{\,2}\, p}{{}^{*}a_x \left(\Sigma_{1x}\right)^2}\right]^2 S_p^{\,2} + \left[\frac{C_3^{\,2}\, p}{{}^{*}a_x \left(\Sigma_{1x}\right)^2}\right]^2 S_p^{\,2}$$

$$= \left[\frac{p}{{}^{*}a_x \left(\Sigma_{1x}\right)^2}\right]^2 C_2^{\,4} + C_3^{\,4} \quad S_p^{\,2} .$$

Now,

$$\left[\frac{S\left({}^{*}a_x\right)}{\left({}^{*}a_x\right)^2}\right]^2 = \left|\frac{p}{C_1^{\,2} - (pC_2)^2 - (pC_3)^2}\right|^2 \left|C_2^{\,4} + C_3^{\,4}\right| S_p^{\,4}$$

$$\frac{S\left({}^{*}a_x\right)}{{}^{*}a_x} = \frac{\sqrt{C_2^{\,4} + C_3^{\,4}}}{\left(\frac{C_1}{p}\right) - C_2^{\,2} - C_3^{\,2}} \left(\frac{S_p}{p}\right)$$

$$\frac{S\left({}^{*}a_x\right)}{{}^{*}a_x} = \frac{\left[\left(\frac{C_2}{C_1}\right)^4 + \left(\frac{C_3}{C_1}\right)^4\right]^{1/2}}{\left(\frac{1}{p}\right)^2 - \left(\frac{C_2}{C_1}\right)^2 - \left(\frac{C_3}{C_1}\right)^2} \left(\frac{S_p}{p}\right) .$$

$\left(\frac{1}{p}\right)^2$ will be much larger than either $\left(\frac{C_2}{C_1}\right)^2$ or $\left(\frac{C_3}{C_1}\right)^2$ .

$$\frac{S\left({}^{*}a_x\right)}{{}^{*}a_x} \cong p^2 \sqrt{\left(\frac{C_2}{C_1}\right)^4 + \left(\frac{C_3}{C_1}\right)^4} \left(\frac{S_p}{p}\right)$$

Table II tabulates $\frac{S\left({}^{*}a_x\right)}{{}^{*}a_x}$ for various values of $\frac{C_2}{C_1}$ and $\frac{C_3}{C_1}$ .

With the assumption that $\frac{C_2}{C_1}$ $\left(\text{and } \frac{C_3}{C_1}\right)$ is uniformly distributed between 1 and 10, the value of error must be calculated as the uncertainty associated with

$$\frac{C_2}{C_1} = 9.5 \quad \cdot \quad \text{(95\% confidence)}$$

TABLE II

TRANSVERSE AXIS CORRECTED ERRORS

| $C_2/C_1$ $(C_3/C_1)$ | $\frac{S\left({}^{*}a_x\right)}{{}^{*}a_x}$ (% RD at 95% confidence) |
|---|---|
| 1 | 0.021 |
| 2 | 0.082 |
| 3 | 0.019 |
| 4 | 0.33 |
| 5 | 0.51 |
| 6 | 0.74 |
| 7 | 1.0 |
| 8 | 1.3 |
| 9 | 1.7 |
| 9.5 | 1.9 |
| 10 | 2.1 |

Transverse axis sensitivity can be an accelerometer measurement problem unless accelerometers are installed in groups of three with the transverse sensitivities known. The data from the triple installation ($C_1$, $C_2$, $C_3$) must then be properly reduced in the data system via equations 1, 2, and 3. The resulting uncertainty in derived acceleration can be considered less than $\pm 1.9\%$ of acceleration reading.

To the extent that transverse-axis-sensitivity compensation is not or cannot be done, larger errors can be anticipated. The controlling equation is

$$C_o = \sqrt{(\Sigma_x a_x)^2 + (\Sigma_y a_y)^2 + (\Sigma_z a_z)^2}$$

with the assumed sensitive axis being the x-axis, for illustration. The apparent error will be:

$$\%\varepsilon = 100\% \ \frac{a_x' - a_x}{a_x}$$

where

$a_x'$ = the apparent x-axis acceleration

$a_x$ = the actual x-axis acceleration.

$$\%\varepsilon = \left[1 - \sqrt{1 + \left(\frac{\Sigma_y a_y}{\Sigma_x a_x}\right)^2 + \left(\frac{\Sigma_z a_z}{\Sigma_x a_x}\right)^2}\right] \times 100\%$$

If, for illustration, we assume

$$\frac{\Sigma_y}{\Sigma_x} = \frac{\Sigma_z}{\Sigma_x} = 0.03 \text{ and } a_y = a_z$$

then

$$\%\varepsilon = \left\{1 - \sqrt{1 + 2\left[(0.03) \ \frac{a_y}{a_x}\right]^2}\right\} \times 100\%$$

$$\%\varepsilon = \left[1 - \sqrt{1 + (0.0018) \ \left(\frac{a_y}{a_x}\right)^2}\right] \times 100\% \quad . \qquad (4)$$

Table III lists %ε for various values of $a_y/a_x$ from Equation (4).

TABLE III

TRANSVERSE AXIS UNCORRECTED ERRORS

| $a_y/a_x$ | 2 axes -% error | 1 axis -% error |
|---|---|---|
| 1 | 0.09 | 0.04 |
| 2 | 0.36 | 0.18 |
| 3 | 0.81 | 0.40 |
| 4 | 1.43 | 0.72 |
| 5 | 2.23 | 1.12 |
| 6 | 3.19 | 1.61 |
| 7 | 4.32 | 2.18 |
| 8 | 5.60 | 2.84 |
| 9 | 7.04 | 3.58 |
| 9.5 | 7.8 | 4.0 |
| 10 | 8.63 | 4.40 |

There are six accelerometer measurements that will be made with one axis measurement missing and one with two axes missing. Though measurements AE-BL4-1 and AE-BL5-1 (on quick-opening valves) are only single-axis measurements, the accelerations anticipated on the uninstrumented axes are expected to be neglibible. For the following seven measurements, the acceleration on the uninstrumented axes may be at least as large as on the instrumented axes.

| | Cross Axis Uncertainty (% RD at 95% confidence) |
|---|---|
| AE-PC10-1 | $\pm 4.0$ |
| AE-PC10-2 | $\pm 4.0$ |
| AE-PC17-1 | $\pm 4.0$ |
| AE-PC17-2 | $\pm 4.0$ |
| AE-BL2-1 | $\pm 4.0$ |
| AE-BL2-2 | $\pm 4.0$ |
| AE-BL3-1 | $\pm 7.8$ |

## 1.2 Base Strain Sensitivity

Piezoelectric accelerometers, will respond fairly readily to direct physical deformation (strain) as well as deformations arising from forces as a result of the acceleration of a seismic mass. For the accelerometers used in LOFT, this sensitivity is 3.9 equivalent $m/s^2$ per 100 $\mu\varepsilon$ (microstrain).

To avoid this measurement problem, LOFT accelerometers are installed on mounting blocks designed to effectively decouple surface strain. This technique (as shown in Figure 5) is used for all of the LOFT accelerometer measurements except AC-BL4-1 and AC-BL5-1 (the two accelerometers on the blowdown valve flanges). In these two installations, the accelerometers are bolted directly to the valve flange.

Study of the specific installation reveals that the total 3 axes vector sum strain in the flange at each mounting location will not exceed 4.3 $\mu\varepsilon$. The nominal base strain sensitivity is 0.04 equivalent $m/s^2$ per $\mu\varepsilon$, and the device range is $\pm 98$ $m/s^2$. This produces an uncertainty due to base strain of

$$4.3 \times 0.04 = \pm 0.17 \text{ m/s}^2 \quad .$$

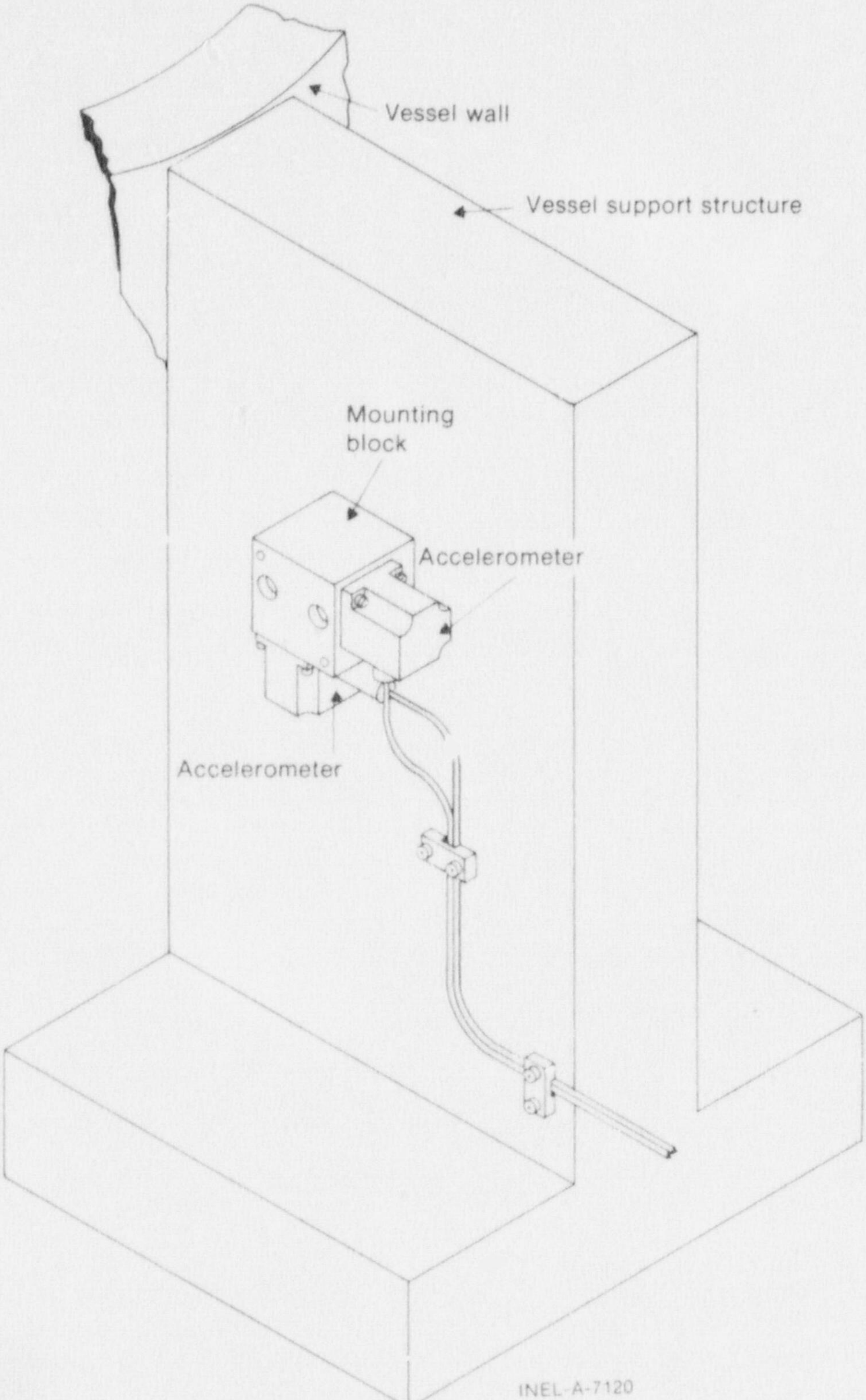


Fig. 5 Typical accelerometer mounting.

## 2. RESPONSE LIMITATIONS

The 10 to 90% rise time of the accelerometer measurement system will be determined by three factors: (a) transducer response, (b) charge amplifier response, and (c) DAVDS multiplex frequency modulation (MFM) system response. The 10 to 90% rise time specified is 1 ms.

A piezoelectric accelerometer is an underdamped system (typical damping is h = 0.05). In a paper by Wood and Cohen[2], the relationship between resonate frequency ($f_r$) and 10 to 90% rise time ($T_R$) is tabulated for various values of damping. For h = 0; $T_r = 0.162/f_r$ and for h = 0.5, $T_R = 0.184/f_r$. Certainly $T_R = 0.184/f_r$ is a pessimistic approximation. Vendor data sheets show all mounted resonant frequencies ($f_r$) to be greater than 8 kHz. This implies that transducer 10 to 90% rise time will certainly be less than 23 μs (15.2 kHz).

Since the signal conditioning is a charge amplifier (integrator) instead of a straight voltage operation amplifier, the cable capacitance connecting the transducer and amplifier will not effect the response time of the measurement system.

Endevco engineers report that the 3-dB frequency for this Endevco Model 2735 charge amplifier is approximately 20 kHz. This is sufficiently above the measurement requirements (350 Hz) as not to be a significant consideration.

The last factor in response time is the DAVDS MFM system. This system has a wideband bandwidth of 1000 Hz, so it will actually be the limiting factor, providing a 10 to 90% rise time of about 0.35 ms.

This generates a combined rise time ($T_c$) of

$$T_c = \sqrt{\begin{pmatrix}\text{transducer}\\ \text{rise time}\end{pmatrix}^2 + \begin{pmatrix}\text{DAVDS}\\ \text{rise time}\end{pmatrix}^2}$$

$$T_c = \sqrt{(0.023)^2 + (0.35)^2} = 0.35 \text{ ms.}$$

## 3. DEPENDENCIES

### 3.1 Temperature

The charge sensitivity temperature coefficient of a piezoelectric accelerometer is variable unit to unit. None of the units tested demonstrate a temperature coefficient in excess of ±1.5% RD per 56 K. The accelerometers are intended to provide data primarily during subcooled decompression, a time (0-100 ms) during which the temperature virtually does not change from its predecompression value. Assuming the temperature can be measured to within ±19 K, the uncertainty attributable to temperature will be ±0.51% RD.

For times after the subcooled decompression or for locations where the steady state temperature differs from the coolant temperature, i.e., AE BL4-1, the equation for correcting the temperature coefficient for temperature is as follows:

$$C = \alpha T + \beta$$

where

$$\alpha = \frac{C_1 - C_2}{\Delta T}$$

$$\beta = C_1 - \frac{T_1}{\Delta T}(C_1 - C_2)$$

C = accelerometer charge sensitivity

$T$ = temperature in K

$C_1$ = charge sensitivity at $T_1$

$C_2$ = charge sensitivity at $T_2$

$\Delta T = T_1 - T_2$.

The following temperatures should be used during subcooled decompression

| Accelerometer | Nonnuclear | Nuclear |
|---|---|---|
| AE BL4-1<br>AE BL5-1<br>AE PC10-1<br>AE PC10-2 | 494 ± 19 K | 533 ± 19 K |
| All other locations | 555 ± 19 K | 589 ± 19 K |

3.2 Frequency

Generally, the performance of an accelerometer is optimized over a specific range of frequencies specified by the user. For LOFT, the reference frequency was chosen to be 100 Hz, with primary use intended from 10 to 1000 Hz. Each accelerometer shows its particular frequency dependence. The response relative to 100 Hz generally falls off by 1 or 2% by 10 Hz and rises by 1 or 2% by 1000 Hz. Using manufacturers' data, the uncertainty in the output dveiations with frequency was determined. This amounts to calculating twice the RSS of all of the deviations, on a lot basis, as at 10, 20, 50, 100, 200, 400, and 1000 Hz. This works out to an uncertainty as a result of frequency dependence of ±1.1% RD for vessel bottom accelerometers and ±0.93% RD for TA accelerometers (based on 23 of the 39 accelerometers). Based on this data a value of ±1% RD will be used as the frequency dependent uncertainty.

## 4. CALIBRATION

The three calibration factors to be contended with are discussed in the following paragraphs. The total RSS calibration uncertainty from these three items is $\pm$1.8% RD.

### 4.1 National Bureau of Standards (NBS) Primary Standard

The NBS estimates the combined uncertainty band on their acceleration standard to be $\pm$0.67% RD.

### 4.2 Gulton's Secondary Standard

This includes the nonstationariness of the reference transducer to NBS as well as environmental, quality control, and any other factors associated with the Gulton factory. This uncertainty is $\pm$1.3% RD.

### 4.3 Linearity

Linearity of the calibration (best-fit straight line) is 1% of reading.

## 5. ELECTRICAL CONSIDERATIONS

There are several electrical aspects associated with the operation of the Endevco 2735 charge amplifier that will cause a signal to show up at the output that does not correlate to charge present at the input.

(1) Common Mode Sensitivity. An assumed common mode interfering signal of $\pm$1 V p-p will cause a $\pm$0.17 $m/s^2$ corruption of the output.

(2) Noise. Random noise referred to output will be only $\pm 0.007$ m/s$^2$.

(3) Linearity. The linearity of the output signal relative to its best-fit straight line is ±0.67% RD.

(4) Total Harmonic Distortion (THD). The THD in the output is ±0.67% RD.

(5) Gain. Gain variations associated with the unpredictable ±10% RD power line variations (105 to 125 volts) will be 0.17% RD.

RSS of (1) and (2) is $\pm 0.17$ m/s$^2$. RSS of (3), (4), and (5) is 0.96% RD.

One potential problem area has been defined in the early LOFT test sequence. The resonant frequency of the accelerometer mentioned in Section III.2 of this report has the potential of causing some loss of data. Although the resonant peak at 8 kHz is outside the bandwidth of interest, the high gain of approximately 50 at the reasonant peak may cause saturation of the wideband input stage of the charge amplifier. To alleviate this problem the input stage of the charge amplifier was set up in the middle rather than the low range, allowing for an increase factor of 10 to the input range. A 1 kHz filter which eliminates the resonant peak is located in the second stage of the charge amplifier. The gain of the buffer amplifier located between the charge amplifier and recording system has been increased to make up the gain loss of the first stage. No significant uncertainty is expected in the final data.

Endevco lists the following maximum charge inputs.

| Range | Maximum Input Charge (pC) | Full Scale ($m/s^2$) | Sensitivity ($pC \cdot s^2/m$) |
|---|---|---|---|
| Low | 3 500 | 10, 300 | 0.1 - 1.0 |
| | | 1.0, 30 | 1.0 - 10 |
| Middle | 35 000 | 1 000, 3 000 | 0.1 - 1.0 |
| | | 100, 300 | 1.0 - 10 |
| High | 100 000 | 10 000, 30 000 | 0.1 - 1.0 |
| | | 1 000, 3 000 | 1.0 - 10 |

## V. SUMMARY OF SPECIFIC UNCERTAINTIES

The measurement uncertainty analysis showed the major sources of uncertainty in the accelerometer were the transverse sensitivity and calibration of the transducers. Anticipated dynamic base strain at two installations (AE-BL4-1 and AE-BL5-1) will cause a slight increase in the uncertainty of these two measurements. The balance of the accelerometers were isolated from change in base strain. A summary of accelerometer uncertainties is given in Table IV. These values are based on a recording range of 98 $m/s^2$.

TABLE IV

SUMMARY OF EXTERNAL ACCELEROMETER UNCERTAINTY ANALYSIS

| Parameter | Uncertainty (95% confidence limits): Vessel bottom and LTA | Uncertainty (95% confidence limits): AE-BL-3-1[b] |
|---|---|---|
| Transverse axis sensitivity | ±4.0% RD | ±7.8% RD |
| Base strain sensitivity | [a] | [a] |
| Temperature | ±0.51% RD | ±0.51% RD |
| Frequency | ±1.0% RD | ±1.0% RD |
| Calibration | ±1.8% RD | ±1.8% RD |
| Electrical considerations | ±0.96% RD | ±0.96% RD |
| plus | ±0.17 $m/s^2$ | ±0.17 $m/s^2$ |
| Measurement channel (RSS) subtotal | ±4.6% RD | ±8.1% RD |
| plus (RSS) | ±0.17 $m/s^2$ | ±0.17 $m/s^2$ |
| DAVDS (MFM) | ±0.94 $m/s^2$ | ±0.94 $m/s^2$ |
| Total (RSS) | ±4.6% RD | ±8.1% RD |
| plus (RSS) | ±0.95 $m/s^2$ | ±0.95 $m/s^2$ |
| Rise time (10 to 90%) | 0.35 ms | |

[a] Negligible, except for AE-BL4-1 and AE-BL5-1 which have ±0.17 $m/s^2$.

[b] Only one axis instrumented.

The MRD requirement[1] for accelerometers is 10% RD. Table IV shows that LOFT experimental accelerometer accuracies are well within this requirement. The uncertainty of AE-BL4-1 and AE-BL5-1 is 8.1% RD plus $\pm 0.97$ m/s$^2$ each. The rise time of the accelerometer itself is 23 μs (15.2 kHz.)

## VI. CONCLUSIONS

The external acceleration measurements will meet MRD requirements[1]. Measurement AE-BL3-1 has only one axis instrumented, making data processing to remove cross axis effects impossible.

Two acceleration measurements (AE-BL4-1 and AE-BL5-1) are being made without using mounting blocks. These two measurements may have additional dynamic base strain effects of $\pm 0.17\ m/s^2$. The ability to calibrate the charge amplifier is the controlling uncertainty.

## VII REFERENCES

1. J. D. Burtt, LOFT Measurement Requirements Document, NUREG/CR-0246, TREE-1197 (July 1978).

2. A. D. Wood and R. Cohen, "Table of Related Characteristics for Second Order Systems", ISA Journal (October 1962).

3. Internal document.

# APPENDIX A

# SPECIFICATIONS

# APPENDIX A

## SPECIFICATIONS

This section consists of a synopsis of performance requirements.

The reactor-vessel-bottom accelerometers (Gulton Model AQB-10180088) were commercially available units. Later, EG&G Idaho specifications were written for the 39 LOFT test assembly (LTA) accelerometers.

## 1.0 EG&G IDAHO REQUIREMENTS

### 1.1 Environment

(1) $10^4$ h at 616 K and atmospheric pressure and humidity, including 100 temperature cycles from room temperature to 616 K.

(2) Neutron flux: $2 \times 10^4$ nv

Integrated: $1.4 \times 10^{11}$ nvt

Gamma flux: $0.5 \times 10^3$ R/h

(3) 100 h at 0.28 MPa, 400 K, and 100% relative humidity.

1.2 Functional and Electrical

| | |
|---|---|
| Acceleration range (minimum): | $\pm 490$ m/s$^2$ |
| Amplitude linearity (of best-fit straight line): | $\pm 1$% |
| Frequency response (minimum): | 2 to $10^3$ Hz, $\pm 5$% |
| Mounted resonant frequency (minimum): | $10^4$ Hz |
| Transverse sensitivity (maximum): | 3% |
| Charge sensitivity (minimum): | 1.0 pC·s$^2$/m |
| Pressure sensitivity: | Output change shall be less than 0.1 m/s$^2$ when transducer is exposed to a pressure change of 0.34 MPa in 0.01 s. |
| Temperature sensitivity (maximum): | $\pm 0.027$%/K |
| Base strain sensitivity (maximum): | 0.04 equivalent m/s$^2$ per microstrain |
| Internal resistance: | 10 megohms minimum at 616 K (higher at lower temperatures) |
| Grounding: | Case shall be isolated from signal ground |

1.3 Other EG&G Idaho requirements included (but not discussed here) are:

(1) Materials

(2) Construction and physical

(3) Cable and cable connectors

## 2.0 VENDOR TRANSDUCER PERFORMANCE

### 2.1 Specifications For Gulton Model AQB-10180088 (reactor vessel bottom).

#### 2.1.1 Operational

| | |
|---|---|
| Charge sensitivity: | 5.1 $pC \cdot s^2/m \pm 10\%$ |
| Internal resistance (@ room temperature): | $2 \times 10^4$ megohms minimum |
| Mounted resonant frequency: | 10 kHz |
| Frequency response ($\pm 5\%$): | 2 Hz to 1 kHz |
| Transverse sensitivity: | 3%, maximum |
| Amplitude linearity: | $\pm 1\%$ of best-fit straight line |
| Temperature response: | $\pm 5\%$, from +200 K to 894 K |

2.1.2 Environmental

| | |
|---|---|
| Temperature range: | 5 to 894 K |

2.1.3 Acceleration Range

| | |
|---|---|
| Vibration: | 1961 $m/s^2$ pk, maximum |
| Shock: | 9810 $m/s^2$, 100 μs, half sine, maximum |
| Humidity: | Hermetically sealed, all welded |
| Altitude: | Unaffected |
| Gamma rates (minimum): | $3.2 \times 10^8$ Rads (c)/h |
| Neutron fluences (minimum): | $9.6 \times 10^{16}$ n/cm |

2.1.4 Physical

| | |
|---|---|
| Operating Mode: | Bolted compression |
| Grounding: | Internally ungrounded |
| Case material: | Stainless steel |
| Mounting: | 3 holes, 0.366-cm inside diameter (ID) on 3.49-cm diameter bolt circle |

| | |
|---|---|
| Weight: | 184 g, maximum |
| Output connector: | Integral stainless steel sheathed, MgO insulated, triaxial, 0.318-cm outside diameter (OD) cable welded into side of transducer case and sealed. Cable length 9.1-m cable terminated with connector. Supply mating connector for all transducers. |
| Dimensions and configurations | 3.81 cm square by 3.81 cm maximum. |

All specifications are nominal unless otherwise indicated.

## 3.0 MEASUREMENT REQUIREMENTS DOCUMENT SPECIFICATION

A complete list of Measurement Requirements Document (MRD)[A-1] acceleration measurement requirements are found in Table II of TREE-NUREG-1089, Volume I. In summary of this listing, there are two acceleration ranges $\pm 4.9$ to 29 $m/s^2$ and $\pm 9.8$ to 98 $m/s^2$; all accuracy requirements are $\pm 10\%$ of reading (RD); all response requirements are 1 ms.

# 4.0 REFERENCES

A-1 J. D. Burtt, LOFT Measurement Requirements Document, NUREG/CR-0246, TREE-1197 (July 1978).

# APPENDIX B

# TEST SIGNAL AMPLITUDE CALCULATIONS

## APPENDIX B

## TEST SIGNAL AMPLITUDE CALCULATIONS

Charge Amplifier Calibration - Endevco Model 2735

Calculate Test Signal Amplitudes

$$E_T = \frac{GS}{C_p + C_c} \text{ volts (peak)}$$

where

$G$ = peak amplitude of measurand ($m/s^2$)

$S$ = charge sensitivity of transducer $pC \cdot s^2/m$

$C_p$ = capacitance of transducer

$C_c$ = capacitance of input cable

(1) External Accelerometer

$G = 392\ m/s^2$

$S = 1.2\ pC \cdot s^2/m$

$C_p = 800$ pF

$C_c = 4550$ pF

$$E_T = \frac{392 \cdot 1.2}{800 + 4550} = 0.089 \text{ V}$$

(2) Vessel Accelerometers (bottom of reactor vessel)

$G = 29\ m/s^2$

$S = 5.1\ pC \cdot s^2/m$

$C_p = 4550$ pF

$C_c = 4550$ pF

$$E_T = \frac{29 \cdot 5.1}{4550 + 4550} = 0.0164 \text{ V}$$

DISTRIBUTION RECORD FOR NUREG/CR-0169, VOL. V
(TREE-1089)

Internal Distribution

1 - Chicago Patent Group - DOE
9800 South Cass
Argonne, IL 60439

2 - R. L. Blackledge
Idaho Operations Office - DOE
Idaho Falls, ID 83401

3 - R. J. Beers, ID

4 - P. E. Litteneker, ID

5 - R. E. Tiller, ID

6 - H. P. Pearson
Information Management, EG&G

7-12 - INEL Technical Library

13-32 - Author

33-88 - Special Internal

External Distribution

89-90 - Saul Levine, Director
Office of Nuclear Regulatory Research, NRC
Washington, D.C. 20555

91-92 - Special External

93-119 - Technical Information Center - DOE
Box 62
Oak Ridge, TN 37830

120-405 - Distribution under R2, Water Reactor Safety Research - Systems Engineering